Chemical Synthesis, in Vitro Acetohydroxyacid Synthase (AHAS) Inhibition, Herbicidal Activity, and Computational Studies of Isatin Derivatives

Jianguo Wang,*,[†] Haizhong Tan,[†] Yonghong Li,[†] Yi Ma,[†] Zhengming Li,[†] and Luke W. Guddat[‡]

[†]State-Key Laboratory and Institute of Elemento-Organic Chemistry, Nankai University, Tianjin 300071, China
[‡]School of Chemistry and Molecular Biosciences, University of Queensland, St. Lucia, Brisbane, QLD 4072, Australia

S *Supporting Information*

ABSTRACT: Acetohydroxyacid synthase (AHAS) catalyzes the first common step in the biosynthesis of the branched-chain amino acids. As a result of its metabolic importance in plants, it is a target for many commercial herbicides. Virtual screening analysis inspired the evaluation of 19 commercially available isatin analogues and 13 newly synthesized isatin derivatives as novel AHAS inhibitors and for their herbicidal activity. The best compound demonstrated 95% inhibition of the activity of *Arabidopsis thaliana* AHAS at a concentration of $100\ mg\ L^{-1}$, whereas the herbicidal activities of three compounds reached 50% inhibition at a concentration of $10\ mg\ L^{-1}$ using the rape root growth test. CoMFA contour models were established to understand the structure−activity relationships for this class of AHAS inhibitor. The compounds were docked to the active site cavity of *A. thaliana* AHAS using FlexX, and the dominant binding mode was consistent with frontier molecular orbital from DFT calculations. This is the first comprehensive study of isatin derivatives as AHAS inhibitors and provides a valuable starting point for the design of new herbicides.

KEYWORDS: AHAS, rational design, synthesis, isatin derivatives, biological activity, herbicide, QSAR, docking, DFT calculation, molecular design

INTRODUCTION

The branched-chain amino acids (BCAAs) can be biosynthesized only by plants and micro-organisms. Animals do not have this ability, obtaining these necessary nutrients from their diet to maintain survival. Thus, enzymes involved in the biosynthesis of the BCAAs are regarded as targets for the development of herbicides or antimicrobial agents.[1] Acetohydroxyacid synthase (AHAS; EC 2.2.1.6, also referred to as acetolactate synthase, ALS) has been a successful herbicidal target for nearly 30 years.[2−4] Four families of AHAS inhibitors that have been widely used as herbicides (Figure 1) are sulfonylureas (SU), imidazolinones (IMI), pyrimidinylthiobenzoates (PTB), and triazolopyrimidine sulfonanilides (TP), and these have contributed enormously to crop protection throughout the world.[5,6] However, with the overuse of these chemicals, resistant weed strains have become a major problem in many areas.[7−11] Thus, there is an urgent need to discover AHAS inhibitors with new chemical structures as potential replacements for those herbicides that are now no longer effective.

The binding modes of the sulfonylureas and one imidazolinone (imazaquin) to AHAS were previously determined by X-ray crystallography.[12−16] These studies have opened the way to the rational design of novel AHAS inhibitors. In 2007, we reported the identification of several novel AHAS inhibitors using virtual screening.[17] Among these was an indigo-based compound, and we hypothesized that the structure of isatin, a half moiety of indigo, might also be active toward AHAS.[17] Thus, we built a library of isatin derivatives to test their inhibition of AHAS and to see if these possess herbicidal activity.

Isatin, a marine natural product, has previously been reported to display significant antifungal activity due to its inhibition of

monoamine oxidase B (MAO-B),[18,19] where it triggers a dose- and time-dependent switch from apoptosis to necrosis in human neuroblastoma cells.[20] Derivatives of isatin can also have anxiogenic, sedative, antitubercular, and anticonvulsant activities and act in vitro as potent antagonists on arterial natriuretic peptide receptors.[21] Herbicidal activities have also been reported for some isatin derivatives.[22−25] However, to date, isatins have not been identified as inhibitors of AHAS. Although a large number of publications and patents describing the synthesis and biological activity of AHAS inhibitors have appeared in the literatures, very few in recent years have identified new lead structures. This paper describes the in vitro and in vivo activity of isatin derivatives as AHAS inhibitors. In addition, three-dimensional (3D) quantitative structure−activity relationship (3D-QSAR) analysis and density functional theory (DFT) calculations have been undertaken to determine the steric, electrostatic, and frontier molecular orbital features that influence the inhibitory activity.

MATERIALS AND METHODS

General Synthesis and Instruments. Compounds **1**−**19** were purchased from Alfa-Aesar or Sigma-Aldrich. Compounds **20**−**32** were synthesized in our laboratory, and the commercial sources of the starting materials were purchased from the Tianjin Guangfu Fine Chemical Research Institute, Alfa-Aesar, or Sigma-Aldrich. The crystal structure of
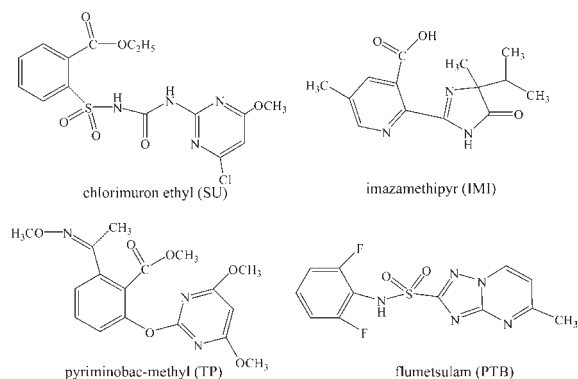
Figure 1. Representative examples of four AHAS inhibitors.

compound **24** has previously been published by our group.[22] All solvents were distilled before use. Melting points were determined using an X-4 melting apparatus and were uncorrected. ^{1}H NMR spectra were obtained using a 300 MHz Bruker AC-P300 spectrometer or a 400 MHz Varian Mercury Plus 400 spectrometer in DMSO-d_6 with TMS as an internal standard. Elemental analyses were determined on a Yanaca CHN Corder MT-3 elemental analyzer. Mass spectra were recorded on a Thermo Finnigan LCQ Advantage LC/mass detector instrument. The control herbicide, monosulfuron, was synthesized in our laboratory as described previously.[26] The structures of all compounds purchased or synthesized are presented in Figure 2. Molecular modeling studies were computed using an SGI 350 server and an SGI Fuel workstation.

Procedures for the Synthesis of Compounds 20–32 (Scheme 1). *Preparation of Compounds 20–23, Example Compound 22.* 3-Fluorobenzoic acid (8.4 g, 60 mmol) was dissolved in anhydrous ethanol (150 mL) in an ice–water bath, and then SOCl$_2$ (7.5 mL, 100 mmol) was added dropwise before stirring for 4 h at 0 °C. Water (50 mL) was then added after the organic solvent, and SOCl$_2$ was removed under vacuum. The pH of the solution was adjusted to 8 by the addition of 1 M NaOH and then extracted with EtOAc. The organic solvent was removed to give the crude product ethyl 3-fluorobenzoate (**a**) (8.24 g, 83%) as a colorless liquid. Hydrazine hydrate (85%, 10 mL) was added to liquid **a** (8.24 g, 50 mmol), and the mixture was refluxed for 6 h before being cooled to room temperature. The product precipitated out of solution after the resulting ethanol was removed. The white crystals were collected by filtration, washed thoroughly with cold EtOAc, and dried to give 3-fluorobenzoylhydrazine (**b**) (5.86 g, 76%). A mixture of chloral hydrate (8.0 mL, 80 mmol) and Na$_2$SO$_4$ (85 g, 600 mmol) was warmed to 40 °C in aqueous solution (180 mL), and then 2-iodoaniline (2.19 g, 10 mmol) in 10% HCl (85 mL) was added dropwise within 0.4 h, and the mixture was stirred for 0.5 h at that temperature. Hydroxylamine hydrochloride (14 g, 200 mmol) was added quickly. The mixture was stirred and heated to 75 °C for 4 h and then cooled to room temperature. The precipitate corresponding to 2′-hydroxyimino-2-iodoacetanilide (**c**) was filtered and dried to give a light-brown solid (18.53 g, 98%). Concentrated sulfuric acid (70 mL) was warmed to 75 °C in a 200 mL flask fitted with an efficient stirrer, and dry **c** (18.53 g, 68 mmol) was added at a suitable speed to keep the temperature between 75 and 80 °C. After that, the solution was heated to 80 °C for 0.5 h to complete the reaction. The reaction mixture was next cooled to room temperature and poured into crushed ice (30 g) with continual stirring. After 1 h, the product was filtered, washed with cold water, and then dried to give a crude red product, 7-iodoindoline-2,3-dione (**d**) (16.12 g, 86%). A mixture of **d** (2.19 g, 8 mmol), **b** (1.23 g, 8 mmol), and acetic acid (2.5 mL) was refluxed in a water/ethanol solution (1:5, 50 mL) for 6 h. The mixture was then cooled to room temperature and a yellow solid precipitated out. The precipitate was filtered, washed with water, dried, and then recrystallized from ethanol to give a pure yellow solid **22**: yield,

57%; mp, 273–274 °C; ^{1}H NMR (DMSO-d_6, 300 MHz), δ 13.82 (s, 1H, NNH), 11.38 (s, 1H, NH), 7.77 (d, 1H, J = 7.8 Hz, Ar$_1$–H4), 7.74–7.54 (m, 5H, 4Ar$_2$–H and Ar$_1$–H6), 6.93 (t, 1H, J = 7.8 Hz, Ar$_1$–H5); ESI-MS, m/z 408 [M − H]$^-$. Anal. Calcd for C$_{15}$H$_9$FIN$_3$O$_2$: C, 44.03; H, 2.22; N, 10.27. Found: C, 43.68; H, 2.47; N, 10.43. The same method was used to synthesize and purify compounds **20**, **21**, and **23**.

Analytical data for compound 20: yellow solid; yield, 65%; mp, 284–286 °C; ^{1}H NMR (DMSO-d_6, 300 MHz), δ 13.76 (s, 1H, NNH), 11.61 (s, 1H, NH), 8.02–7.42 (m, 6H, 4Ar$_2$–H and Ar$_1$–H4, Ar$_1$–H6), 7.06 (t, 1H, J = 8.1 Hz, Ar$_1$–H5); ESI-MS, m/z 360 [M − H]$^-$. Anal. Calcd for C$_{15}$H$_9$BrFN$_3$O$_2$: C, 49.75; H, 2.50; N, 11.60. Found: C, 49.49; H, 2.68; N, 11.82.

Analytical data for compound 21: brown–yellow solid; yield, 66%; mp, 287–289 °C; ^{1}H NMR (DMSO-d_6, 300 MHz), δ 13.81 (s, 1H, NNH), 11.68 (s, 1H, NH), 7.73–7.53 (m, 6H, 4Ar$_2$–H and Ar$_1$–H4, Ar$_1$–H6), 7.08 (t, 1H, J = 7.8 Hz, Ar$_1$–H5); ESI-MS, m/z 360 [M − H]$^-$. Anal. Calcd for C$_{15}$H$_9$BrFN$_3$O$_2$: C, 49.75; H, 2.50; N, 11.60. Found: C, 49.56; H, 2.78; N, 11.71.

Analytical data for compound 23: yellow solid; yield, 60%; mp, 291–293 °C; ^{1}H NMR (DMSO-d_6, 400 MHz), δ 11.76 (s, 1H, NNH), 11.12 (s, 1H, NH), 8.00 (d, 1H, J = 8 Hz, Ar$_2$–H3), 7.72 (d, 1H, J = 8 Hz, Ar$_1$–H4), 7.59–6.97 (m, 5H, Ar$_2$–H4, Ar$_2$–H5, Ar$_2$–H6 and Ar$_1$–H6, Ar$_2$–OH), 6.90 (t, 1H, J = 7.6 Hz, Ar$_1$–H5); ESI-MS m/z 406 [M − H]$^-$. Anal. Calcd for C$_{15}$H$_{10}$IN$_3$O$_3$: C, 44.25; H, 2.48; N, 10.32. Found: C, 44.52; H, 2.39; N, 10.17.

Preparation of Compounds 24–26, Example Compound 24. A mixture of 3-chloro-2-hydrazinylpyridine (**e**) (1.15 g, 8 mmol), isatin (1.18 g, 8 mmol), and acetic acid (2.5 mL) was refluxed in a water/ethanol solution (1:5, 40 mL) for 6 h. The mixture was then cooled to room temperature and an orange solid precipitated out. The precipitate was filtered, washed with water, dried, and recrystallized from ethanol to give yellow crystals. Analytical data for compound **24** have been previously reported.[22] The intermediates **e**, **f**, and **g** were synthesized by using a previously described method.[27−29] The same method was used to synthesize and purify compounds **25** and **26**.[22]

Analytical data for compound 25: yellow solid; yield, 67%; mp, 256–258 °C; ^{1}H NMR (DMSO-d_6, 300 MHz), δ 12.75 (s, 1H, NNH), 11.27 (s, 1H, NH), 7.57 (br s, 1H, Ar–H4), 7.39 (t, 1H, J = 7.5 Hz, Ar–H6), 7.10 (t, 1H, J = 7.2 Hz, Ar–H5), 6.94 (d, 1H, J = 7.2 Hz, Ar–H7), 5.87 (s, 1H, Het–CH), 5.36 (s, 1H, COCH$_2$), 5.01 (s, 1H, COCH$_2$), 2.19 (s, 3H, Het–CH$_3$), 2.10 (s, 3H, Het–CH$_3$); ESI-MS m/z 296 [M − H]$^-$. Anal. Calcd for C$_{15}$H$_{15}$N$_5$O$_2$: C, 60.60; H, 5.09; N, 23.56. Found: C, 60.33; H, 5.12; N, 23.27.

Analytical data for compound 26: yellow solid; yield, 67%; mp, 265–266 °C; ^{1}H NMR (DMSO-d_6, 400 MHz), δ 12.95 (s, 1H, NNH), 11.31 (s, 1H, NH), 7.61 (d, 1H, J = 7.6 Hz, Ar–H4), 7.39 (t, 1H, J = 7.6 Hz, Ar–H6), 7.12 (t, 1H, J = 7.6 Hz, Ar–H5), 6.94 (d, 1H, J = 7.6 Hz, Ar–H7), 2.69–2.67 (br s, 6H, Het–2CH$_3$); ESI-MS, m/z 299 [M−H]$^-$. Anal. Calcd for C$_{14}$H$_{12}$N$_4$O$_2$S: C, 55.99; H, 4.03; N, 18.65. Found: C, 55.89; H, 3.91; N, 18.29.

Preparation of Compounds 27–32, Example Compound 28. To a solution of ethyl benzoate (22.53 g, 150 mmol) in anhydrous ethanol (65 mL) was added 85% hydrazine hydrate (35 mL). The resulting mixture was refluxed for 4 h and then cooled to room temperature. The product precipitated out of solution, white crystals were collected by filtration, and these were washed with cold water and dried to give benzhydrazide (**h**) (18.5 g, 90%). A mixture of isatin (0.59 g, 4 mmol) and potassium carbonate (2.5 g, 18 mmol) was heated at 65 °C in DMF (30 mL). After 1 h, 1-(chloromethyl)-3-fluorobenzene (0.58 g, 4 mmol) was added in portions, and the stirring was continued at 65 °C until no isatin was detectable (TLC). The mixture was then cooled to room temperature and poured into water (60 mL) with continual stirring. After 40 min, 1-(3-fluorobenzyl)indoline-2,3-dione (**i**) was filtered, washed with cold water, and then dried to give a crude red product,
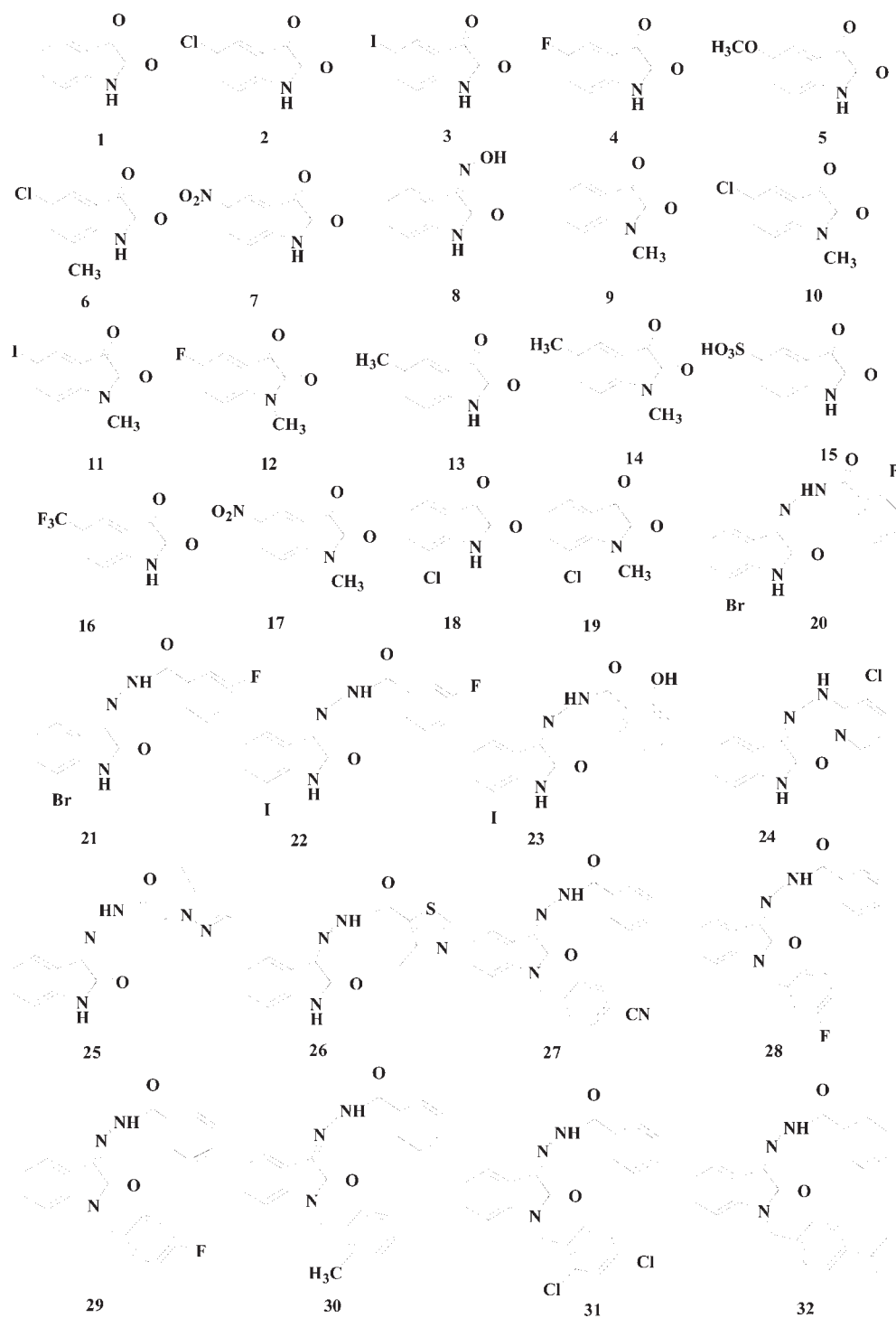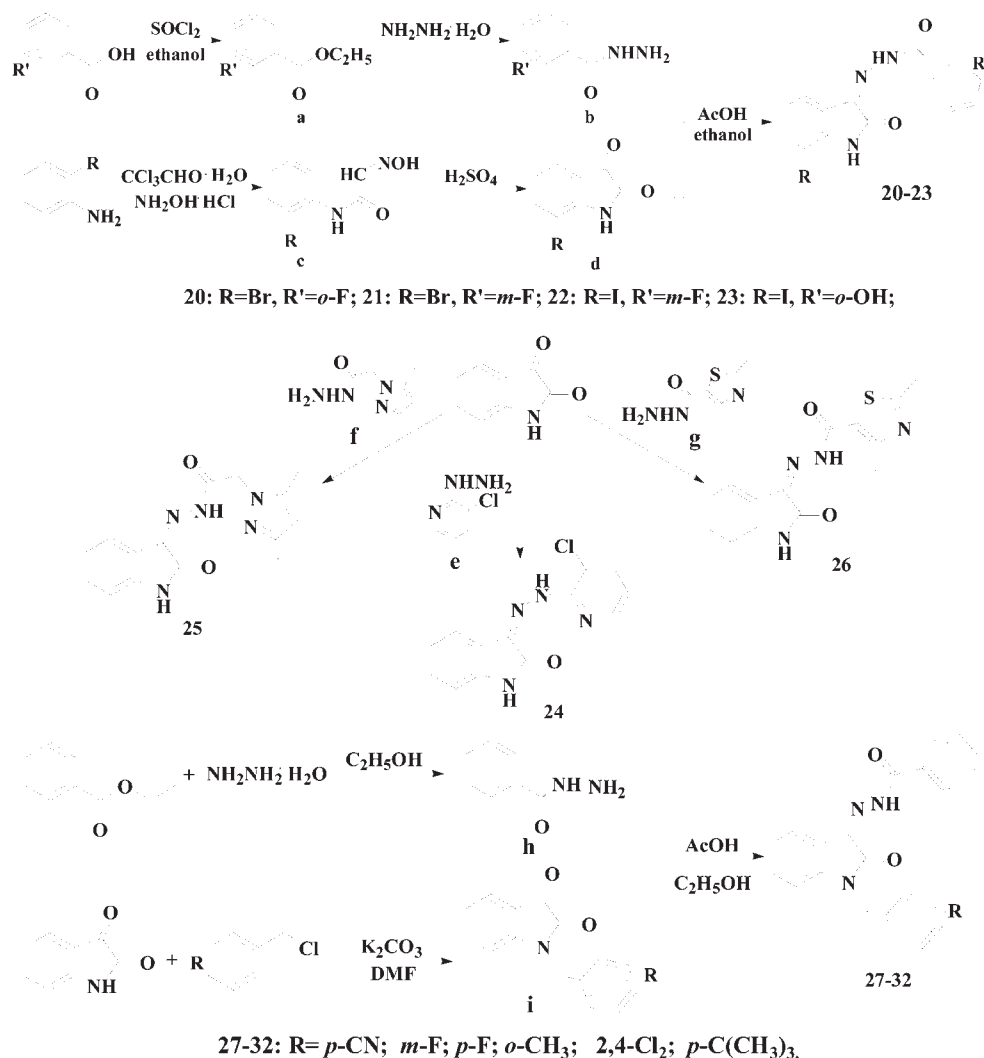
Figure 2. Structures of isatin (compound **1**) and derivatives tested in this study as novel AHAS inhibitors.

purified by flash column chromatography on silica gel (0.82 g, 80%), the eluting solvent for which is ethyl acetate/petroleum ether (1:3). A mixture of **h** (0.51 g, 2 mmol), **I**, and acetic acid (1.0 mL) was refluxed in a water/alcohol solution (1:5, 25 mL) for 5 h. The reaction mixture was next cooled to room temperature and a yellow solid precipitated out. This precipitate was filtered, washed with water, and then dried to give a crude yellow product. Recrystallization from ethanol gave pure yellow solid **28**: yield, 71%; mp, 165−166 °C; ^{1}H NMR (DMSO-d_6, 400 MHz), δ 13.84 (s, 1H, NNH), 7.94 (d, 2H, J = 6.8 Hz, Ar_2−H2 and

Ar_2−H6), 7.73−7.10 (m, 10H, 4 Ar_3−H, Ar_2−H3, Ar_2−H4, Ar_2−H5, Ar_1−H4, Ar_1−H5, and Ar_1−H6), 7.07 (d, 1H, J = 7.6 Hz, Ar_1−H7), 5.05(s, 2H, Ar_3−CH_2N); ESI-MS, m/z 372 [M − H]⁻. Anal. Calcd for $C_{22}H_{16}FN_3O_2$: C, 70.77; H, 4.32; N, 11.25. Found: C, 70.42; H, 4.39; N, 11.11. The same method was used to synthesize and purify compounds **27** and **29−32**.

*Analytical data for compound **27***: yellow solid; yield, 98%; mp, 242−243 °C; ^{1}H NMR (DMSO-d_6, 300 MHz), δ 13.81 (s, 1H, NNH), 7.94 (d, 2H, J = 7.8 Hz, Ar_2−H2 and Ar_2−H6), 7.83 (d, 2H, J = 8.4 Hz,

Scheme 1. Synthetic Routes for New Isatin Derivatives 20−32

20: R=Br, R'=*o*-F; 21: R=Br, R'=*m*-F; 22: R=I, R'=*m*-F; 23: R=I, R'=*o*-OH;

27-32: R= *p*-CN; *m*-F; *p*-F; *o*-CH₃; 2,4-Cl₂; *p*-C(CH₃)₃.

Ar₃−H3 and Ar₃−H5), 7.71−7.60 (m, 6H, Ar₃−H2, Ar₃−H6, Ar₂−H3, Ar₂−H4, Ar₂−H5, and Ar₁−H4), 7.42 (t, 1H, J = 7.8 Hz, Ar₁−H6), 7.19 (t, 1H, J = 7.5 Hz, Ar₁−H5), 7.06 (d, 1H, J = 8.1 Hz, Ar₁−H7), 5.13 (s, 2H, Ar₃−CH₂N); ESI-MS, m/z 379 [M − H]⁻. Anal. Calcd for C₂₃H₁₆N₄O₂: C, 72.62; H, 4.24; N, 14.73. Found: C, 72.88; H, 4.39; N, 14.76.

*Analytical data for compound **29**:* light-yellow solid; yield, 92%; mp, 213−214 °C; ¹H NMR (DMSO-d₆, 400 MHz), δ 13.85 (s, 1H, NNH), 7.94 (d, 2H, J = 7.6 Hz, Ar₂−H2 and Ar₂−H6), 7.73−7.16 (m, 10H, 4 Ar₃−H, Ar₂−H3, Ar₂−H4, Ar₂−H5, Ar₁−H4, Ar₁−H5, and Ar₁−H6), 7.10 (d, 1H, J = 8.0 Hz, Ar₁−H7), 5.01 (s, 2H, Ar₃−CH₂N); ESI-MS, m/z 372 [M − H]⁻. Anal. Calcd for C₂₂H₁₆FN₃O₂: C, 70.77; H, 4.32; N, 11.25. Found: C, 70.88; H, 4.48; N, 11.59.

*Analytical data for compound **30**:* orange solid; yield, 88%; mp, 187−188 °C; ¹H NMR (DMSO-d₆, 300 MHz), δ 13.86 (s, 1H, NNH), 7.93 (d, 2H, J = 8.1 Hz, Ar₂−H2 and Ar₂−H6), 7.72−7.08 (m, 9H, 4 Ar₃−H, Ar₂−H3, Ar₂−H4, Ar₂−H5, Ar₁−H4, and Ar₁−H6), 7.06 (t, 1H, J = 7.8 Hz, Ar₁−H5), 6.96 (d, 1H, J = 7.8 Hz, Ar₁−H7), 5.01 (s, 2H, Ar₃−CH₂N), 2.40 (s, 3H, Ar₃−CH₃); ESI-MS, m/z 368 [M − H]⁻. Anal. Calcd for C₂₃H₁₉N₃O₂: C, 74.78; H, 5.18; N, 11.37. Found: C, 74.51; H, 5.08; N, 11.29.

*Analytical data for compound **31**:* yellow solid; yield, 85%; mp, 202−204 °C; ¹H NMR (DMSO-d₆, 300 MHz), δ 13.77 (s, 1H, NNH), 7.92 (d, 2H, J = 6.9 Hz, Ar₂−H2 and Ar₂−H6), 7.73−7.30 (m, 8H, 3Ar₃−H, Ar₂−H3, Ar₂−H4, Ar₂−H5, Ar₁−H4, and Ar₁−H6), 7.21 (t, 1H, J = 7.5 Hz, Ar₁−H5), 6.99 (d, 1H, J = 7.8 Hz, Ar₁−H7), 5.07 (s, 2H, Ar₃−CH₂N); ESI-MS, m/z 422 [M − H]⁻. Anal. Calcd for C₂₂H₁₅Cl₂N₃O₂: C, 62.28; H, 3.56; N, 9.90. Found: C, 62.07; H, 3.66; N, 9.70.

*Analytical data for compound **32**:* yellow solid; yield, 59%; mp, 171−172 °C; ¹H NMR (DMSO-d₆, 300 MHz), δ 13.87 (s, 1H, NNH), 7.94 (d, 2H, J = 7.2 Hz, Ar₂−H2 and Ar₂−H6), 7.71−7.17 (m, 10H, 4Ar₃−H, Ar₂−H3, Ar₂−H4, Ar₂−H5, Ar₁−H4, Ar₁−H5, and Ar₁−H6), 7.14 (d, 1H, J = 7.5 Hz, Ar₁−H7), 4.98 (s, 2H, Ar₃−CH₂N), 1.24 (s, 9H, Ar₃−C(CH₃)₃); ESI-MS, m/z 411 [M − H]⁻. Anal. Calcd for C₂₆H₂₅N₃O₂: C, 75.89; H, 6.12; N, 10.21. Found: C, 75.66; H, 5.95; N, 10.20.

Biological Assays. *Determination of Inhibition of Arabidopsis thaliana AHAS (AtAHAS).* The expression and purification of *At*AHAS has been described previously.[30] AHAS activity was measured using the colorimetric assay in a previous publication.[17]

In Vivo Inhibition of the Root Growth of Rape (Brassica campestris L). The in vivo data were determined using our previously published method.[31]

Molecular Modeling. *CoMFA.* Chemical structures of the compounds were built within Sybyl 7.3 (Tripos Inc., St. Louis, MO). All of the molecules were assigned MMFF94 charges and minimized by the Tripos force field when convergence reached 0.001 kcal mol⁻¹ Å⁻¹.

Table 1. In Vitro and in Vivo Biological Activity of the Isatins

| | AtAHAS inhibition (%) | | rape root length inhibition (%) | |
no.	100 mg L^{-1}	D	100 mg L^{-1}	10 mg L^{-1}
1	70 ± 3	6.14	52 ± 2	24 ± 1
2	55 ± 4	6.69	95 ± 1	28 ± 2
3	70 ± 3	6.94	92 ± 2	31 ± 3
4	65 ± 2	6.39	88 ± 2	52 ± 1
5	60 ± 2	6.57	30 ± 3	20 ± 1
6	65 ± 3	6.60	65 ± 2	10 ± 1
7	60 ± 3	6.68	82 ± 1	7 ± 1
8	45 ± 3	6.72	55 ± 2	0
9	50 ± 4	6.62	24 ± 1	7 ± 2
10	60 ± 3	6.70	53 ± 1	20 ± 1
11	60 ± 3	7.21	27 ± 2	13 ± 1
12	60 ± 2	6.59	59 ± 1	19 ± 2
13	50 ± 3	6.61	80 ± 1	13 ± 2
14	75 ± 5	6.26	26 ± 1	14 ± 2
15	10 ± 2	8.02	18 ± 3	4 ± 1
16	60 ± 3	6.83	93 ± 1	27 ± 2
17	25 ± 3	7.42	33 ± 1	2 ± 1
18	70 ± 4	6.41	83 ± 2	51 ± 2
19	80 ± 4	6.27	59 ± 2	31 ± 2
20	95 ± 2	6.40	39 ± 1	14 ± 1
21	60 ± 3	7.50	16 ± 3	0
22	75 ± 3	7.35	81 ± 1	51 ± 1
23	95 ± 1	6.55	25 ± 1	0
24	70 ± 3	6.94	19 ± 1	0
25	35 ± 2	7.69	27 ± 2	0
26	30 ± 2	7.75	21 ± 3	0
27	20 ± 1	8.34	48 ± 1	2
28	95 ± 3	6.44	40 ± 1	0
29	80 ± 3	7.11	15 ± 2	0
30	50 ± 3	7.71	0	0
31	50 ± 2	7.89	6 ± 1	0
32	60 ± 3	7.67	15 ± 1	0
C*[a]	90 ± 1		78 ± 1	64 ± 2

[a] C*, control herbicide, monosulfuron.

The molecules were superimposed using isatin (1) as the template. Comparative molecular field analysis (CoMFA) was used for the 3D-QSAR analysis using default parameters.[32] The "leave-one-out" (LOO) cross-validation method was applied to determine the optimum number of partial least-squares (PLS) components. The biological activities were expressed in terms of D (Table 1) using the formula[33−35]

$$D = \log_{10}[a/(1 - a)] + \log_{10} M_w$$

where a is the percent inhibition of AHAS in vitro, M_w is the molecular weight of the inhibitor, and D is the biological activity index.

DFT Calculation. Representative compounds 6, 20, and 29 were chosen for DFT geometry optimization by the SCF method using the B3LYP (Becke, three-parameter, Lee−Yang−Parr) function with a basis set of 6-31 G(d) to describe their molecular properties.[36,37] Gaussian03 was used to perform the calculations.[38] The initial conformations were chosen from the structural database for CoMFA. All computations were conducted for the ground states of these molecules as singlet states. All of the convergent precisions used were the system's default values. The frontier molecular orbital (HOMO-k, k = 0, 1, 2 and LUMO+k, k = 0, 1,

2; HOMO, highest occupied molecular orbital; LUMO, lowest unoccupied molecular orbital) was calculated precisely. Frequency analysis was performed, and partial atomic charges were derived from a population analysis based on the natural bond orbital (NBO) method.[38]

Molecular Docking. The molecular docking of the isatins to AHAS was performed by FlexX.[39] The crystal structure of AtAHAS in complex with chlorimuron ethyl (pdb code 1YBH) was retrieved from the pdb databank.[6] All amino acids in the protein were modified in the "Biopolymer" module to correct side-chain rotamer conformations. All water molecules were removed, and hydrogen atoms were added in the standard geometry. Any amino acid residue within 6.5 Å of the location of the chlorimuron ethyl was considered to be in the binding pocket. Cscore calculation was enabled and set to serial mode. Database docking and subsequent scoring procedures were performed using the default parameters of FlexX within Sybyl7.3. The figures were generated by PYMOL (DeLano Scientific, South San Francisco, CA) and Chem-Draw (ACD Laboratories, Toronto, Canada).

■ RESULTS AND DISCUSSION

Synthetic Chemistry of the Title Compounds. Compounds 20−32 were synthesized by a mild condensation reaction from indoline-2,3-dione (or substituted) and a substituted hydrazine in the presence of acetic acid in ethanol solution under refluxing conditions and gave favorable yields. The synthetic methods for the intermediates in Scheme 1 are detailed under Materials and Methods. It should be noted that it is theoretically possible for both the E and Z isomers for every Schiff base to be synthesized. However, for all of the title compounds only a single isomer was obtained. From selected X-ray structures of isatin Schiff bases,[22,40,41] all of the molecules exist as Z isomers so that an intramolecular hydrogen bond is formed between the isatin unreacted carbonyl oxygen atom and the hydrogen atom bonded to the nitrogen atom in the hydrazone group. This forms a large π electron conjugate plane (formed by the three connected rings) stabilizing the molecule. The identities and structures of all the compounds synthesized were determined by ESI-MS, elemental analysis, and ^{1}H NMR.

Biological Activity. The in vitro and in vivo biological activities of the 32 isatin derivatives are summarized in Table 1. The in vitro activity was evaluated at a concentration of 100 mg L^{-1} against AtAHAS, whereas the in vivo activity was measured using the rape root inhibition method developed at Nankai University.[42] The sulfonylurea herbicide monosulfuron was used as the control. These results show that most of the compounds exhibited considerable in vitro and in vivo inhibitory activities. The most potent of the compounds, 20, 23, and 28, showed 95% in vitro inhibition against AtAHAS at a concentration of 100 mg L^{-1}. At the same concentration monosulfuron inhibited the activity of AtAHAS by 90%. In the rape root test these three compounds were not as potent as expected, with no more than 40% inhibition of growth at a concentration of 100 mg L^{-1}, compared with 78% for monosulfuron. On the other hand, compounds 2−4, 7, 13, 16, 18, and 22 displayed 80−95% inhibition of rape root growth at 100 mg L^{-1}, which are values better than that observed for monosufuron. It is encouraging that compounds 4, 18, and 22 showed ∼50% in vivo inhibition at 10 mg L^{-1}, whereas at this level monosufuron reduced the in vivo activity by 63.8%. Compounds 4, 18, and 22 were able to inhibit AtAHAS by 65, 70, and 75%, respectively.

Reports dating back to 1957 indicate that isatins can have herbicidal activity, although the mechanism of action for these compounds is unknown.[23−25] It has previously been demonstrated

9896

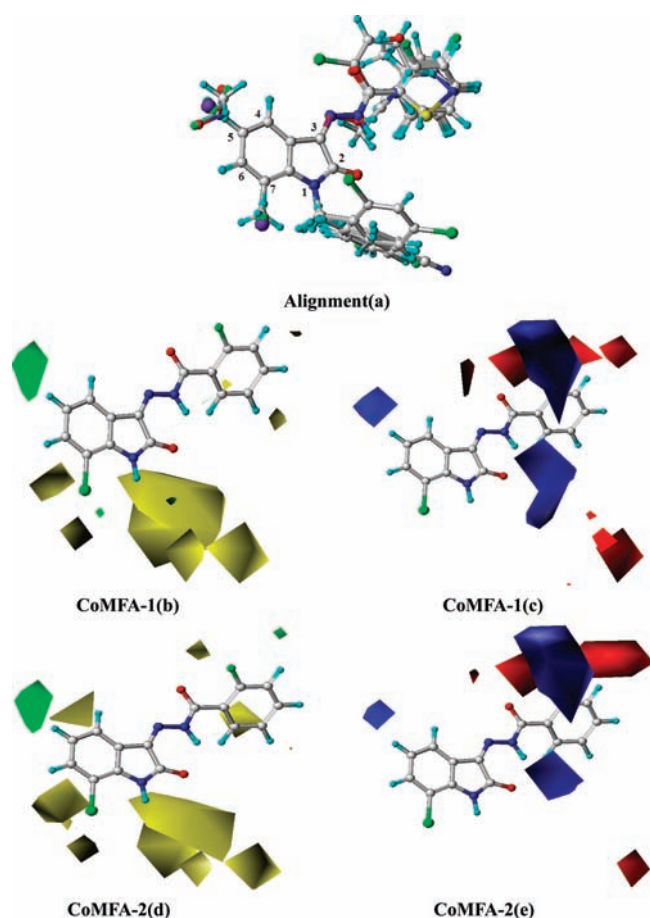dx.doi.org/10.1021/jf2021607 |J. Agric. Food Chem. 2011, 59, 9892–9900

Figure 3. (a) Alignment of the isatins in the training set for CoMFA analysis with the numbers of positions: (b—e) ball and stick model of compound **20**; (b, d) steric contour maps for the CoMFA models (sterically favored and disfavored regions are shown in green and yellow, respectively); (c, e) electrostatic contour maps for the CoMFA models (positively charged favored regions are shown in blue, and negatively charge favored regions are shown in red).
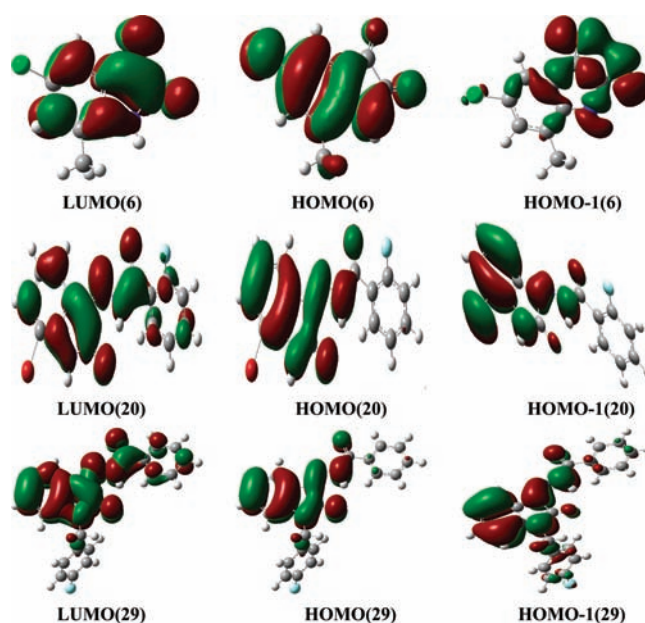

Figure 4. LUMO, HOMO, and HOMO-1 maps for compounds **6**, **20**, and **29** from DFT calculations. The green parts represent positive molecular orbital, and the red parts represent negative molecular orbital.

that inhibition of AHAS by the sulfonylureas (and all of the compounds in Figure 1) is the basis for their herbicidal activity.[31] The data in Table 1 show that isatin inhibitors of AtAHAS also exhibit herbicidal activity, suggesting that their activity is due to their inhibition of AHAS. Further studies are required to confirm the linkage between the herbicidal activity of isatins and their inhibition of AtAHAS. Such experiments may include control in vivo rape root length studies in the presence of BCAA.

The current isatins have weaker in vivo activity than many of the commercial sulfuonylurea herbicides, but the discovery of a new family of AHAS inhibitors is of major significance, particularly in view of the emergence of weeds resistant to many of the currently available AHAS inhibitors. Further structural optimization of the isatins should therefore be undertaken.

CoMFA Results and the 3D Contour Models. For computational analysis all of the molecules were built as the Z isomer. Compounds **14**, **15**, **17**, **30**, and **32** were excluded from the database because they were statistical outliers in the training set. The inclusion of any of these molecules did not yield a satisfactory leave-one-out q^2. The best score that could be obtained was <0.3. However, the leave-one-out q^2 is 0.498 when using five optimum components (CoMFA-1) and is 0.535 when using six optimum

components (CoMFA-2), with standard errors of prediction (SEP) of 0.431 and 0.425, respectively. Both values are acceptable considering the fairly large molecular diversity of the isatin training set. The PLS statistics of all CoMFA models and the figures for predicted activity versus experimental activity can be found in the Supporting Information. The alignment of compounds in the training set and 3D contour maps for CoMFA-1 and CoMFA-2 are shown in Figure 3. Compound **20** was used to illustrate the structure—activity relationships. The CoMFA-1 and CoMFA-2 3D contour models are very similar, suggesting that for this training set, using five components is acceptable. For the steric contour map (Figure 3b,d), the green region displays a position where a bulky group would be favorable for higher AtAHAS inhibition; this region is located at the 5-position of the isatin ring. The sterically unfavorable region is in yellow, and this is mostly near the 1- and 7-positions of the isatin ring. For the electrostatistic contour map (Figure 3c,e), the blue contour defines a region where an increase in the positive charge will result in an increase in affinity, whereas the red contour defines a region of space where negative charge is favorable. From the maps, it can be observed that the electrostatically favored region is located near the 5-position of isatin and projects forward of the 3-position. An electrostatically disfavored region projects behind the 3-position and is far from the 1- and 2-positions of isatin. On the basis of these results it will be possible to design and synthesize more potent isatin inhibitors of plant AHAS.

DFT Calculation. Frontier molecular orbital theory should be taken into account when structure—activity relationships are investigated because the HOMO and LUMO make significant contributions to ligand—enzyme interactions.[43−45] We therefore calculated the frontier molecular orbital of representative compounds **6**, **20**, and **29** that have good AtAHAS inhibition by means of DFT/B3LYP. LUMO+1, LUMO+2, and HOMO-2 maps did not give useful information. However, meaningful results were observed from LUMO, HOMO, and HOMO-1 maps (Figure 4). In all of the frontier molecular orbital maps, it
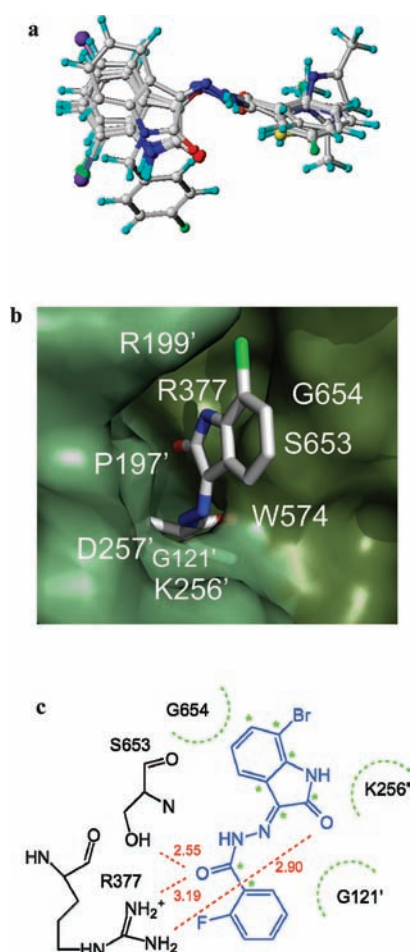
Figure 5. FlexX docking of isatins to *At*AHAS: (a) overlay of docked conformations for compounds **1**, **3**, **20**−**22**, **25**, **26**, and **29**; (b) Connolly surface of *At*AHAS with compound **20** shown as a stick model (the two subunits of *At*AHAS are in different shades of green); (c) hydrogen bonds between the enzyme and inhibitor shown as red dashed lines and distances in Å units, amino acid residues within van der Waals contact of compound **20** shown as green arcs, an atom belonging to compound **20** that participates in van der Waals attractions to the enzyme identified by green star. Residues labeled with a prime are from an alternate subunit that completes the active site.

can be seen that the isatin moiety in all of the molecules makes a major contribution to the binding of *At*AHAS. These are largely through π−π or hydrophobic interactions and are most obvious in the HOMO maps. The frontier molecular orbital maps show that the carbonyl positioned adjacent to the hydrazone nitrogen atom also plays an important role in binding, especially for compounds **20** and **29**. It is interesting to note that for compound **29**, only a small portion of the frontier molecular orbital spreads into the adjacent aromatic ring at the 1-postion of isatin, indicating that the group at the 1-position plays a very minor role. Thus, it can be concluded that the isatin moiety makes a significant contribution to the binding to *At*AHAS.

Molecular Docking. All of the isatins were docked to the binding site of *At*AHAS by using the program FlexX. Compounds **1**, **3**, **20**−**22**, **25**, **26**, and **29** all adopt a similar conformation and location in the active site (Figure 5a), whereas none of the other 24 compounds yielded consistent docking poses. Figure 5b shows the docking of compound **20** in the

binding site of *At*AHAS, demonstrating that the inhibitor fits neatly into the binding cavity. A two-dimensional representation shows which atoms of the inhibitor interact directly with *At*AHAS (Figure 5c). The diagram emphasizes that hydrophobic contacts to the protein are through the indole moiety and the carbonyl carbon atom in the bridge. This is in good agreement with the observations from the frontier MO and DFT results. From Figure 5c it can be observed that the inhibitor makes hydrophobic contact with the G654, K256, and G121 of *At*AHAS. Hydrogen bonds are also observed between the carbonyl oxygen of compound **20** and the side chains of S653 and R377.

The location of compound **20** when docked to the surface of *At*AHAS resembles that of the sulfonylureas in that it is bound to an area referred to as the herbicide binding site, which is located directly above the active site. With this site filled by an inhibitor it is not possible for the substrate to gain access to the active site to allow catalysis to occur. In common between the structures of the sulfonylureas and compound **20** is that they both possess two aromatic rings and a bridge that links them together. In both cases, the rings are orthogonal to each other due to the bending of the bridge within the herbicide binding site. Another similarity is that two residues, R377 and S653, form hydrogen bonds to the bridge sections of both inhibitors. However, there are also some differences when the molecular modeling results of the docked isatins into the crystal structure of *At*AHAS are compared with the crystal structures of the sulfonlyureas or imazaquin when in complex with this enzyme.[15] For example, in the crystal structures, W574 is crucial for the sulfonylurea to form π−π stacking, whereas compound **20** does not make such an interaction with this residue. Additionally, D376 and M200 do not make any contacts with compound **20**, yet both play important roles when binding with the sulfonylureas or imazaquin. The side chain of R199 forms part of the surface where compound **20** is bound, but does not participate directly in any noncovalent ligand−enzyme interactions (Figure 5b,c). It will be interesting to compare the binding affinities of the isatins to those of mutant AHAS enzymes, whereby resistance to the sulfonylureas or imidizolinones has already developed. In particular, the W574L mutation is the most commonly observed resistant biotype found in field isolates. Because the isatins do not bind directly to W574, we would anticipate that the isatins are inhibitors of this variant.

In summary, 32 isatin derivatives were assessed as novel AHAS inhibitors both in enzymatic assays and in the rape root growth test. The combination of 3D-QSAR, DFT calculation, and molecular docking provided meaningful clues as to the structural features of this new family of AHAS inhibitors that are important for binding and will help in the design of more potent compounds in the future.

■ ASSOCIATED CONTENT

Ⓢ Supporting Information. Predicted activities versus experimental activities of isatins and PLS statistics of CoMFA models for isatins. This material is available free of charge via the Internet at http://pubs.acs.org.

■ AUTHOR INFORMATION

Corresponding Author
*Phone: +86-(0)22-23499414. Fax: +86-(0)22-23503627. E-mail: nkwjg@nankai.edu.cn.

9898

dx.doi.org/10.1021/jf2021607 |*J. Agric. Food Chem.* 2011, 59, 9892–9900

■ REFERENCES

(1) Duggleby, R. G.; Pang, S. S. Acetohydroxyacid synthase. *J. Biochem. Mol. Biol.* **2000**, *33* (1), 1–36.

(2) Chaleff, R. S.; Mauvais, C. J. Acetolactate synthase is the site of action of two sulfonylurea herbicides in higher plants. *Science* **1984**, *224*, 1443–1445.

(3) LaRossa, R. A.; Schloss, J. V. The sulfonylurea herbicide sulfometuron methyl is an extremely potent and selective inhibitor of acetolactate synthase in *Salmonella typhimurium*. *J. Biol. Chem.* **1984**, *259*, 8753–8757.

(4) Ray, T. B. Site of action of chlorsulfuron: inhibition of valine and isoleucine biosynthesis of plants. *Plant Physiol.* **1984**, *75*, 827–831.

(5) Whitcomb, C. E. An introduction to ALS-inhibiting herbicides. *Toxicol. Ind. Health* **1999**, *15* (1−2), 231–239.

(6) McCourt, J. A.; Duggleby, R. G. Acetohydroxyacid synthase and its role in the biosynthetic pathway for branched-chain amino acids. *Amino Acids* **2006**, *31*, 173–210.

(7) Tan, S.; Evans, R. R.; Dahmer, M. L.; Singh, B. K.; Shaner, D. L. Imidazolinone-tolerant crops: history, current status and future. *Pest. Manag. Sci.* **2005**, *61* (3), 246–257.

(8) Moss, S. R. Herbicide-resistant weeds in Europe: the wider implications. *Commun. Agric. Appl. Biol. Sci.* **2004**, *69* (3), 3–11.

(9) Gressel, J. Crops with target-site herbicide resistance for *Orobanche* and *Striga* control. *Pest. Manag. Sci.* **2009**, *65* (5), 560–565.

(10) Green, J. M.; Hazel, C. B.; Forney, D. R.; Pugh, L. M. New multiple-herbicide crop resistance and formulation technology to augment the utility of glyphosate. *Pest. Manag. Sci.* **2008**, *64* (4), 332–339.

(11) Corbett, C. A.; Tardif, F. J. Detection of resistance to acetolactate synthase inhibitors in weeds with emphasis on DNA-based techniques: a review. *Pest. Manag. Sci.* **2006**, *62* (7), 584–597.

(12) Pang, S. S.; Duggleby, R. G.; Guddat, L. W. Crystal structure of yeast acetohydroxyacid synthase: a target for herbicidal inhibitors. *J. Mol. Biol.* **2002**, *317*, 249–262.

(13) Pang, S. S.; Guddat, L. W.; Duggleby, R. G. Molecular basis of sulfonylurea herbicide inhibition of acetohydroxyacid synthase. *J. Biol. Chem.* **2003**, *278*, 7639–7644.

(14) McCourt, J. A.; Pang, S. S.; Guddat, L. W.; Duggleby, R. G. Elucidating the specificity of sulfonylurea herbicide binding to acetohydroxyacid synthase. *Biochemistry* **2005**, *44*, 2330–2338.

(15) McCourt, J. A.; Pang, S. S.; King-Scott, J.; Guddat, L. W.; Duggleby, R. G. Herbicide binding sites revealed in the structure of plant acetohydroxyacid synthase. *Proc. Natl. Acad. Sci. U.S.A.* **2006**, *103*, 569–573.

(16) Wang, J. G.; Lee, P.; Dong, Y. H.; Pang, S. S.; Duggleby, R. G.; Li, Z. M.; Guddat, L. W. Crystal structures of two novel sulfonylurea herbicides in complex with *Arabidopsis thaliana* acetohydroxyacid synthase. *FEBS. J.* **2009**, *276*, 1282–1290.

(17) Wang, J. G.; Xiao, Y. J.; Li, Y. H.; Ma, Y.; Li, Z. M. Identification of some novel AHAS inhibitors via molecular docking and virtual screening approach. *Bioorg. Med. Chem.* **2007**, *15* (1), 374–380.

(18) Gil-Turnes, M. S.; Hay, M. E.; Fenical, W. Symbiotic marine bacteria chemically defend crustacean embryos from a pathogenic fungus. *Science* **1989**, *246*, 116–118.

(19) Binda, C.; Li, M.; Hubalek, F.; Restelli, N.; Edmondson, D. E.; Mattevi, A. Insights into the mode of inhibition of human mitochondrial monoamine oxidase B from high-resolution crystal structures. *Proc. Natl. Acad. Sci. U.S.A.* **2003**, *100* (17), 9750–9755.

(20) Igosheva, N.; Lorz, C.; O'Conner, E.; Glover, V.; Mehmet, H. Isatin, an endogenous monoamine oxidase inhibitor, triggers a dose- and time-dependent switch from apoptosis to necrosis in human neuroblastoma cells. *Neurochem. Int.* **2005**, *47*, 216–224.

(21) Surendra, N. P.; Sivakumar, S.; Mayank, J.; Seshaiah, K. S. Biological activities of isatin and its derivatives. *Acta Pharm.* **2005**, *55*, 27–46.

(22) Tan, H. Z.; Wang, W. M.; Shang, J. L.; Song, H. B.; Li, Z. M.; Wang, J. G. Syntheses, crystal structures and bioactivities of two isatin derivatives. *Chinese J. Struct. Chem.* **2011**, *30* (4), 502–507.

(23) Haga, T.; Nagano, H.; Enomoto, M.; Morita, K.; Sato, M. Preparation of isatin derivatives as herbicides. Jpn. Patent 63313770, 1988.

(24) Schreiber, K.; Stephan, U.; Wegner, G. Agent for controlling the growth of clover, especially red clover. Ger. Patent DD121011, 1976.

(25) Hambsch, E. Isatins as selective herbicides. Ger. Patent DE1013469, 1957.

(26) Wang, J. G.; Ma, N.; Wang, B. L.; Wang, S. H.; Song, H. B.; Li, Z. M. Synthesis, crystal structure and biological activity of *N*-(4-methylpyrimidin-2-yl)-*N′*-2-(nitrophenylsulfonyl)urea and its docking with yeast AHAS. *Chinese J. Org. Chem.* **2006**, *26* (5), 648–652.

(27) Dulin, W. E.; Wright, J. B. Dulin, W. E.; Wright, J. B. U.S. Patent 3150148, 1964

(28) Cooper, M.; Receveur, J.-M.; Hoegberg, T.; Nielsen, P. A.; Linget, J.-M.; Noeregaard, P. K. Preparation of pyrazolecarboxamide compounds as CB1 receptor modulators. PCT Int. Appl. WO 2008074982, 2008

(29) Platonova, O. V.; Volkova, S. B.; Malin, S. A.; Veretennikov, E. A.; Laskin, B. M.; Malin, A. S. Synthesis of new substituted thiazoles containing aminooxadiazole ring. *Russ. J. App. Chem.* **2008**, *81* (3), 513–515.

(30) Chang, A. K.; Duggleby, R. G. Herbicide-resistant forms of *Arabidopsis thaliana* acetohydroxyacid synthase: characterization of the catalytic properties and sensitivity to inhibitors of four defined mutants. *Biochem. J.* **1998**, *333*, 765–777.

(31) Wang, J. G.; Li, Z. M.; Ma, N.; Wang, B. L.; Jiang, L.; Pang, S. S.; Lee, Y. T.; Guddat, L. W.; Duggleby, R. G. Structure-activity relationships for a new family of sulfonylurea herbicides. *J. Comput.-Aided Mol. Des.* **2005**, *19* (11), 801–820.

(32) Cramer, M.; Cramer, R. D.; Jones, D. M. Comparative molecular field analysis. 1. Effect of shape on binding of steroids to carrier proteins. *J. Am. Chem. Soc.* **1988**, *110*, 5959–5967.

(33) Zhu, Y. Q.; Wu, C.; Li, H. B.; Zou, X. M.; Si, X. K.; Hu, F. Z.; Yang, H. Z. Design, synthesis, and quantitative structure—activity relationship study of herbicidal analogues of pyrazolo[5,1-*d*][1,2,3,5]tetrazin-4(3*H*)ones. *J. Agric. Food Chem.* **2007**, *55* (4), 1364–1369.

(34) Wang, L.; Ma, Y; Liu, X. H.; Li, Y. H.; Song, H. B.; Li, Z. M. Synthesis, herbicidal activities and comparative molecular field analysis study of some novel triazolinone derivatives. *Chem. Biol. Drug Des.* **2009**, *73* (6), 674–681.

(35) Wang, J. G.; Fu, X. L.; Wang, Y. M.; Ma, Y.; Li, Z. M.; Zhang, Z. X. 3D-QASR sudy of quinoline-2,4-dione derivatives against wheat leaf rust. *Chem. J. Chinese Univ.* **2003**, *24* (11), 2010–2013.

(36) Becke, A. D. Density-functional thermochemistry. III. The role of exact exchange. *J. Chem. Phys.* **1993**, *98*, 5648–5652.

(37) Lee, C.; Yang, W.; Parr, R. G. Development of the Colle—Salvetti correlation-energy formula into a functional of the electron density. *Phys. Rev. B* **1988**, *37*, 785–789.

(38) Frisch, M. J.; Trucks, G. W.; Schlegel, H. B.; Scuseria, G. E.; Robb, M. A.; Cheeseman, J. R.; Montgomery, J. A., Jr.; Vreven, T.; Kudin, K. N.; Burant, J. C.; Millam, J. M.; Iyengar, S. S.; Tomasi, J.; Barone, V.; Mennucci, B.; Cossi, M.; Scalmani, G.; Rega, N.; Petersson, G. A.; Nakatsuji, H.; Hada, M.; Ehara, M.; Toyota, K.; Fukuda, R.; Hasegawa, J.; Ishida, M.; Nakajima, T.; Honda, Y.; Kitao, O.; Nakai, H.; Klene, M.; Li, X.; Knox, J. E.; Hratchian, H. P.; Cross, J. B.; Adamo, C.; Jaramillo, J.; Gomperts, R.X; Stratmann, R. E.; Yazyev, O.; Austin, A. J.; Cammi, R.; Pomelli, C.; Ochterski, J. W.; Ayala, P. Y.; Morokuma, K.; Voth, G. A.; Salvador, P.; Dannenberg, J. J.; Zakrzewski, V. G.; Dapprich, S.; Daniels, A. D.; Strain, M. C.; Farkas, O.; Malick, D. K.; Rabuck, A. D.;

9899

dx.doi.org/10.1021/jf2021607 |*J. Agric. Food Chem.* 2011, 59, 9892–9900

Raghavachari, K.; Foresman, J. B.; Ortiz, J. V.; Cui, Q.; Baboul, A. G.; Clifford, S.; Cioslowski, J.; Stefanov, B. B.; Liu, G.; Liashenko, A.; Piskorz, P.; Komaromi, I.; Martin, R. L.; Fox, D. J.; Keith, T.; AlLaham, M. A.; Peng, C. Y.; Nanayakkara, A.; Challacombe, M.; Gill, P. M. W.; Johnson, B.; Chen, W.; Wong, M. W.; Gonzalez, C.; Pople, J. A. *Gaussian 03*, revision C01; Gaussian, Inc.: Wallingford, U.K., 2004.

(39) Rarey, M.; Kramer, B.; Lengauer, T.; Klebe, G. A fast flexible docking method using an incremental construction algorithm. *J. Mol. Biol.* **1996**, *261*, 470–489.

(40) Sun, Y.; Lu, J.; Zhang, D.; Song, H. Synthesis and crystal structure of isatin-3-isonicotinoylhydrazone. *Anal. Sci.* **2006**, *22*, 237–238.

(41) Sandra, S.; Konstantinović; Agneš, K.; Blaga, C.; Radovanović; Andrea, D. Synthesis, X-ray and antimicrobial activity of isatin-3-phenylhydrazone. *CI&CEQ* **2008**, *14* (1), 27–34.

(42) Wang, B. L.; Duggleby, R. G.; Li, Z. M.; Wang, J. G.; Li, Y. H.; Wang, S. H.; Song, H. B. Synthesis, crystal structure and herbicidal activity of mimics of intermediates of the KARI reaction. *Pest Manag. Sci.* **2005**, *61* (4), 407–412.

(43) Huang, X.; Liu, T; Gu, J.; Luo, X.; Ji, R.; Cao, Y.; Xue, H.; Wong, J. T.; Wong, B. L.; Pei, G.; Jiang, H.; Chen, K. 3D-QSAR model of flavonoids binding at benzodiazepine site in GABAA receptors. *J. Med. Chem.* **2001**, *44*, 1883–1891.

(44) Ma, Y.; Wang, J. G.; Wang, B.; Li, Z. M. Integrating molecular docking, DFT and CoMFA/CoMSIA approaches for a series of naphthoquinone fused cyclic α-aminophosphonates that act as novel topoisomerase II inhibitors. *J. Mol. Model.* **2011**, *17* (8), 1899–1909.

(45) Liu, X. H.; Chen, P. Q.; Wang, B. L.; Li, Y. H.; Wang, S. H.; Li, Z. M. Synthesis, bioactivity, theoretical and molecular docking study of 1-cyano-N-substituted-cyclopropanecarboxamide as ketol-acid reductoisomerase inhibitor. *Bioorg. Med. Chem. Lett.* **2007**, *17* (13), 3784–3788.